Multi-modal Brain Tensor Factorization: Preliminary Results with AD Patients

Göktekin Durusoy[1], Abdullah Karaaslanlı[1], Demet Yüksel Dal[1],
Zerrin Yıldırım[2], and Burak Acar[1(✉)]

[1] Department of Electrical and Electronics Engineering, VAVlab,
Boğaziçi University, Istanbul, Turkey
{goktekin.durusoy,abdullah.karaaslanli,demet.yuksel,acarbu}@boun.edu.tr
[2] Aziz Sancar Experimental Medical Research Institute,
Department of Neuroscience, Istanbul University, Istanbul, Turkey
yildirimzerrin@gmail.com

Abstract. Global brain network parameters suffer from low classification performance and fail to provide an insight into the neurodegenerative diseases. Besides, the variability in connectivity definitions poses a challenge. We propose to represent multi-modal brain networks over a population with a single 4D brain tensor ($\mathbf{B}$) and factorize $\mathbf{B}$ to get a lower dimensional representation per case and per modality. We used 7 known functional networks as the canonical network space to get a 7D representation. In a preliminary study over a group of 20 cases, we assessed this representation for classification. We used 6 different connectivity definitions (modalities). Linear discriminant analysis results in 90–95% accuracy in binary classification. The assessment of the canonical coordinates reveals Salience subnetwork to be the most powerful in classification consistently over all connectivity definitions. The method can be extended to include functional networks and further be used to search for discriminating subnetworks.

Keywords: Functional networks · Tensor factorization
Structural networks · Brain connectome · Alzheimer's Disease

1 Introduction

Brain has been known to be a network of cortical regions, yet until the relatively recent advances in magnetic resonance imaging (MRI), it was not possible to build network models of in-vivo brain. Current functional MRI (fMRI) and diffusion MRI (dMRI) technologies allow us to delineate functional (fNET) and structural network (sNET) models, collectively called the brain connectome, at a cortical parcellation scale. The analysis of these network models has the potential of shedding light on how the brain works, as well as the cause and progress of neurodegenerative diseases.

The majority of the analysis approaches has been focused on the changes in the global network features, such as the clustering coefficient, the average path-length, the small-worldness index, etc. Despite their high sensitivity to abnormalities, these features are poor in classification and/or staging due to their global nature [1]. A more promising approach is to assess the changes in sub-networks of the connectome, towards which purely statistical techniques, such as Network Based Statistics (NBS) [2], have gained popularity. Another concern is the lack of standardized techniques for building connectomes, which introduces an unavoidable uncertainty on the derived conclusions.

We propose to use the powerful tensor factorization techniques to simultaneously address the aforementioned problems, namely sub-network based and multi-modal analysis of the connectome. We introduce the *Brain Tensor* (**B**-tensor) as a multi-dimensional multi-modal connectome representation and factorize it in terms of apriori known *canonical subnetwork*s. In a preliminary study with Alzheimer's Disease patients, we demonstrate that the factorization coefficients not only have high discrimination power in a binary classification task, but also provide an insight into the most affected/discriminative canonical subnetworks. We conclude with a discussion on the potential extensions of **B**-tensor factorization.

2   Background

Initial efforts on network analysis have focused on global, and local characteristics in order to identify components of networks, and to assess similarities or differences between networks. Utilizing global features such as clustering coefficients, average path length, small-worldness is useful when a given network is compared with a reference network, or to examine differences of neural networks from different species. Briefly, global features look at the network as a whole and fail to identify local difference. On the other hand, local features such as local clustering coefficient, shortest path etc. have shown their significance when properties of individual components are examined [3].

NBS has been proposed to overcome the limitation of global assessment. It identifies statistically significantly different edges between two classes of networks. The identified edges are used to detect discriminative subnetworks. The distribution of sizes of these subnetworks is used to assign a p-value to the sub-network identified as discriminative between the positive classes. NBS is purely statistical, oversees the a priori known structure of brain.

Karahan et al. utilized coupled tensor factorization to fuse EEG, FMRI, and DTI data represented in 3rd, 2nd, and 3rd order tensors, respectively. Coupling is enforced over temporal and spatial domains for EEG/FMRI and over subjects for EEG/DTI. Two different representation is used for EEG where first one is time-varying and the other one is subject-varying EEG [4]. However, in this research, a priori is not used and multimodal structural and functional representation of brain networks have not been considered. Utilized tensors do not represent network sets row signals/spectra with a spatial and/or subject dimension. Williams et al. generate a 3rd order tensor model by using a trial-structured

neural data with dimensions represent neurons, time and trials. With the help of TCA (Tensor Component Analysis), they have managed to decompose this tensor into three interpretable factors (neuron factors, temporal factors, trial factors). In addition, TCA has been utilized for dimension reduction [5].

We propose a 4th order **B**-tensor that represents multi-modal networks (structural and/or functional) over a population. A modality is defined as a network construction method independent from data source (i.e. structural or functional data). Decomposition of **B**-tensor over a priori known subnetwork is studied.

3 Method

3.1 B-Tensor Construction

For a multi-modal (R-modal) connectome defined over $I \times J$ nodes (cortical parcels) for a population of K cases, the 4th order B-tensor ($\mathbf{B} \in \mathbb{R}^{K \times I \times J \times R}$) is defined. In this work, we used 6 variants of sNET definitions, hence $R = 6$, over a population of 20 cases, hence $K = 20$. We used the 148-parcel Destrieux atlas [6], hence $I = J = 148$.

Following the co-registration of T1-weighted MRI and dMRI volumes, the T1-weighted MRI volume is parcellated using FreeSurfer[1], into 148 parcels which are used to define the 148 nodes ($\{V_i\}$) of the sNETs. Diffusion tensor (DT) volume is computed from diffusion weighted MRI (DWI) using an in-house software built upon the MITK platform[2]. Fiber tracts are constructed using the 4th-order Runge-Kutta (RK4) deterministic tractography algorithm [7] with minimum fractional anisotropy (FA) set to 0.15, stepsize set to 0.7 mm ($\approx$ half the voxel size), minimum fiber length set to 14 mm and the maximum curvature set to 35°. RK4 was initiated from 30 randomly selected seeds per voxels with $FA > 0.15$.

In order to construct the sNETs, each fiber ($\{f_k\}$) is associated with the nodes in the vicinity of its end-points using a symmetric 3D Gaussian kernel with a standard deviation (σ) of 0.155 mm, centered at the fiber endpoints. σ is optimized by minimizing the integrated square error (ISE), as described in [8]. The numeric volumetric integral of the Gaussian kernel positioned at one of the end points of f_k, within the node V_i (and up to a radial distance of 2σ) is used as the fiber-parcel/node association and is denoted by W_{ik}.

Six different sNETs are constructed using 6 different structural connectivity (network edge weight) definitions, C_{ij}, between pairs of nodes, (V_i, V_j), as follows:

$$C_{ij} = \sum_k W_{ik} W_{jk} : \text{Weighted Connectivity} \qquad (1)$$

$$C_{ij}^N = \frac{2 \times \frac{C_{ij}}{\mathcal{V}}}{V_i + V_j} : \text{Normalized Connectivity} \tag{2}$$

$$C_{ij}^{stat} = \frac{1}{C_{ij}} \sum_k W_{ik} W_{jk} \times \Psi(FA(f_k(t))) \ , \ \forall C_{ij} \neq 0$$

$$\text{FA-based Connectivities} \tag{3}$$

where $\mathcal{V}$ is the voxel volume in mm^3, V_i and V_j are the volumes of corresponding parcels, and Ψ represents the statistics operator ($\in$\{min, max, mean, median\}) operating over the fiber parametrized by t.

3.2   B-Tensor Factorization

The CP factorization of $\mathbf{B}$ is given as [9,10],

$$\mathbf{B}_{k,i,j,r} \approx \sum_{q=1}^{Q} \mathbf{A}_{k,q} \mathbf{C}_{i,q} \mathbf{D}_{j,q} \mathbf{E}_{r,q} \tag{4}$$

where the decomposition is performed over Q (free parameter) factors. Each one of the components represents the factorization of a single dimension of $\mathbf{B}$ over the Q factors. While $\mathbf{A}$ and $\mathbf{E}$ are associated with the individual cases and the sNET definitions, $\mathbf{C}$ and $\mathbf{D}$ are solely associated with the network topology. Hence, we combined $\mathbf{C}$ and $\mathbf{D}$ into a single component that represents network topologies across Q factors, while $\mathbf{A}$ and $\mathbf{E}$ are merged to represent per case per connectivity (per-modality) represented in terms of those network topologies. Namely,

$$\mathbf{B}_{k,i,j,r} \approx \sum_{q=1}^{Q} \mathbf{M}_{k,r,q} \mathbf{G}_{i,j,q} = \sum_{q=1}^{Q} \left(\sum_s \mathbf{A}_{k,s} \mathbf{E}_{r,s} \mathbf{I}_{q,s} \right) \left(\sum_s \mathbf{C}_{i,s} \mathbf{D}_{j,s} \mathbf{I}_{q,s} \right) \tag{5}$$

where $\mathbf{I}_{q,s} = \delta_{qs}$, i.e. the identity matrix and $s \in \{1, 2, \cdots, Q\}$. This allows us to decouple the network topology from the cases and the modalities (connectivity definitions). Thus, we can work with case and modality independent network topologies, namely the *canonical subnetworks*, $\mathbf{G}$. With a further simplification, we constrained $\mathbf{G}$ to be a binary valued tensor representing the apriori known (fixed) canonical subnetworks. Following Yeo et al., we defined 7 canonical subnetworks, namely the visual, the somatomotor and auditory, the dorsal attention, the salience, the limbic, the frontoparietal and the default mode subnetworks [11]. They are expressed in terms of the node definitions of $\mathbf{B}$ and numbered from 1 to 7, respectively. $\mathbf{G}$ is assumed known and fixed for the rest. $\mathbf{M}$, on the other hand, represents the factorization coefficients over the canonical dimensions (subnetworks). This gives us 7D representations per case and per modality as $\mathbf{F}_{k,r} \in \mathbb{R}^7$.

Following [12], Eq. 5 can be matricised as

$$\mathbf{B}_{(1,4;2,3)} = \mathbf{M}_{(3;1,2)}^T \mathbf{G}_{(3;1,2)} \tag{6}$$

where $\mathbf{M}_{(3;1,2)} = \mathbf{M}_{(3)} = (\mathbf{E} \odot \mathbf{A})^T$ and $\mathbf{G}_{(3;1,2)} = (\mathbf{G}_{(3)} = \mathbf{D} \odot \mathbf{C})^T$.[3] Fixing $\mathbf{G}$ as described above, we can solve for $\mathbf{M}$ using any matrix inversion technique, such as QR decomposition, to get $\mathbf{M}_{(3)} = \mathbf{G}_{(3)}^{-T}\mathbf{B}_{(1,4;2,3)}^T$. $\mathbf{G}_{(3)}^{-T}$ is computed once and used throughout the analysis. Finally, the computed $\mathbf{M}_{(3)}$ is tensorized back to its original form to get the estimated $\mathbf{M}$ as a 3rd order tensor representing per case, per connectivity unconstrained real-valued factorization coefficients.

4   Experiments

4.1   Data

T1-weighted MRI and dMRI images were acquired by using a Philips Achieva 3.0T X scanner with a 32-channel head coil from 7 AD patients and 13 controls with written consent. The AD patients were diagnosed by means of standard clinical evaluation tests by a team of expert neurologists. We used 3D FFE (Fast Field Echo) pulse sequence with multi-shot TFE (Turbo Field Echo) imaging mode for T1-weighted MRI. The acquisition parameters were TE/TR = 3.8ms/8.3ms, flip-angle = 8°, SENSE reduction 2 (Foot-Head), FOV = $220(RL) \times 240(AP)\,\text{mm}^2$, voxel size = $1.0 \times 1.0 \times 1.0\,\text{mm}^3$ and number of slices = 180. dMRI were acquired with a maximum gradient strength of 40 mT/m, and 200 mT/m/ms slew rate, using a single-shot, pulse-gradient spin echo (PGSE), echo planar imaging (EPI) sequence. The acquisition parameters were FOV= $200 \times 236\,\text{mm}^2$, 2.27 mm isotropic voxel size, 112×112 reconstruction matrix, 71 slices and $TE/TR = 92\,\text{ms}/9032\,\text{ms}$. 120 diffusion weighting gradient directions were used at various b-values between $3000 - 0\,\text{s/mm}^2$.

4.2   Analysis and Results

The separation of the AD patients and the controls in the 7D canonical space of subnetworks was assessed by Linear Discriminant Analysis(LDA) [13]. Binary classifiers are trained for each one of the 6 connectivity definitions in the corresponding 7D space ($\mathbf{F_r}$) and the training accuracies are measured. We also computed the unit normal of separating hyperplanes, i.e. the *canonical axis*, along which the separation of the two groups is maximized. Acc_B represents the binary classification accuracy. We also trained a separate binary classifier using LDA on the standard global network parameters (global clustering coefficients [14], average shortest path length [15], small-worldness index [16]). Acc_{glb} represents the classification accuracy using these global parameters. The results are given in Table 1 together with the corresponding canonical axes for the B-tensor analysis. All accuracies were above 90%, with the weighted and normalized connectivity definitions being the best performing ones for $\mathbf{B}$-tensor. The corresponding classification accuracies using global connectome features in LDA are between 75%–90%.

---

[3] $\odot$ denotes the Khatri-Rao product.

Table 1. Classification accuracies of LDA classifier for different connectivity definitions (modalities) and the associated canonical axes.

Conn	Canonical Axis	Acc_B	Acc_{glb}
C_{ij}	[0.012 −0.010 −0.377 −0.887 0.211 −0.159 −0.022]	0.95	0.8
C_{ij}^N	[−0.326 −0.130 −0.530 −0.636 0.426 0.054 −0.073]	0.95	0.85
C_{ij}^{min}	[−0.224 −0.064 −0.351 −0.509 0.401 0.448 −0.446]	0.90	0.75
C_{ij}^{max}	[−0.352 0.231 −0.345 −0.703 0.299 0.056 0.340]	0.90	0.90
C_{ij}^{mean}	[−0.352 −0.287 −0.298 −0.714 0.347 0.046 0.215]	0.90	0.80
C_{ij}^{median}	[−0.333 −0.296 −0.286 −0.741 0.347 0.0461 0.215]	0.90	0.75

The components of the canonical axes unit vectors provide an insight with regard to the relevance of the corresponding canonical subnetwork in discriminating the AD patients from the controls. The higher the absolute value of a component of a canonical axes, the more important that canonical dimension (subnetwork) is in discriminating the two groups. Figure 1 shows the mean and standard deviation of the magnitude of each component computed over all modalities.

In order to compare the connectivity definitions with regard to their discriminating power, we ordered the canonical subnetworks based on the mean values given in Fig. 1 and computed the classification accuracy of LDA using the top K ($\in [1, 7]$) canonical subnetworks, separately for each connectivity definition. Figure 2 shows the results. In general, increasing the dimension of the canonical space improves the accuracy, except for the 2D case (i.e. using the dorsal
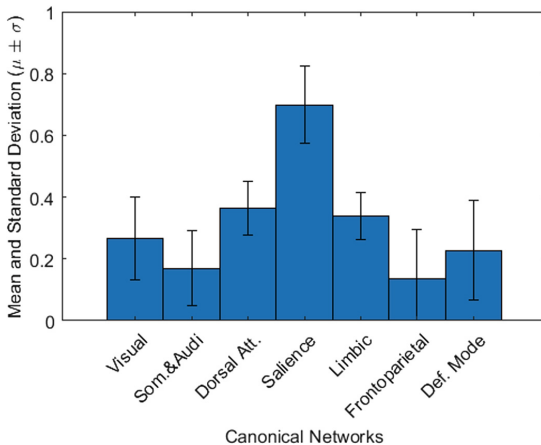
Fig. 1. Mean and standard deviations of the canonical axes' components computed over all modalities. The 4th subnetwork (Salience subnetwork) is consistently observed to be the most important one.
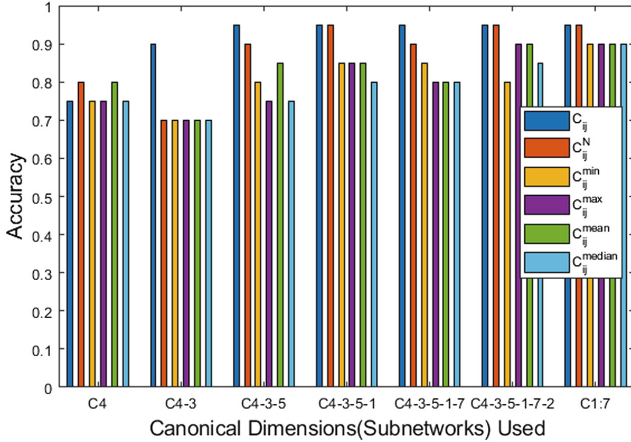
Fig. 2. Accuracy of LDA for all modalities using top K ($\in [1, 7]$) canonical dimensions (subnetworks). The weighted connectivity definition performed the best almost unanimously where as the FA-statistics based connectivities performed relatively poorly in general.

attention and the salience networks only). However, the weighted connectivity definition performed the best almost unanimously where as the FA-statistics based connectivities performed relatively poorly in general.

5   Discussion

The B-tensor factorization allows us to represent the multi-modal (multi-connectivity) brain connectome in a canonical space of subnetworks with an intuitive interpretation. The AD patients are clearly separated from the controls in this space. The salience network is consistently observed to be the most important subnetwork among the 7 subnetworks used. The dorsal attention and the limbic subnetworks seem to be the second most important networks whereas the fronto-parietal network is the least important one. Although this result seems to be counter intuitive as the memory loss (primary function of limbic subnetwork) is the major symptom of AD, there is also evidence supporting our findings [17]. Furthermore, the AD cases in our dataset are described as early stage AD by our collaborating neurologists, which may also explain the observed importance of the salience subnetwork. These preliminary results are limited by the fixed definition of the canonical subnetworks. However, the B-tensor factorization framework can be utilized for searching for discriminative subnetworks. This would provide a further insight into the causes and progression mechanism of neurodegenerative diseases.

The assessment of different connectivity definitions within the aforementioned canonical space reveals that the weighted and normalized connectivity

definitions' discriminative power outperforms those of FA-statistics based connectivities. Although it has been discussed that the FA is an indirect measure of the quality of communication between cortical regions, these preliminary results suggest the opposite. This is potentially due to well-known deficiencies of diffusion tensor model that underlies the FA measurements. A similar assessment using the microstructural integrity of the fiber tracts by means of compartment models, such as NODDI [18], can potentially show a higher discriminative power.

The continuous representation of brain connectome in the canonical space can also be used for staging the disease progression. A regression analysis between this low-dimensional representation and clinical test results should be carried out, which is left for future work. Current study is limited to different sNET definitions, yet the framework is suitable to include fNETs in the B-tensor simultaneously with sNETs. Such a multi-modal analysis may uncover non-trivial relations between the structural and functional changes during the course of the disease, by means of the correlations of different modalities as represented in the canonical space. A fundamental limitation of the present study is the small dataset size which might have caused an overfitting of the LDA classifier. Further experiments on a larger dataset are due to arrive at stronger conclusions.

6   Conclusion

We have presented a novel tensor based multi-modal representation of brain connectome and described how it can be factorized to get a continuous, low-dimensional representation in a canonical space offering an intuitive understanding of neurodegenerative diseases' causes and progression. Preliminary results with a small cohort of AD patients and controls revealed high classification accuracy and identified the salience subnetwork as the most discriminative network component among the 7 known.

Future work will include the experiments with a larger cohort, the extension of the model to joint analysis of structural and functional networks, the assessment of the canonical representation as a disease staging/monitoring biomarker and developing a canonical subnetwork search strategy optimized for classification/regression accuracy.

References

1. Fornito, A., Zalesky, A., Bullmore, E.T.: Fundamentals of Brain Network Analysis. Academic Press, San Diego (2016)
2. Zalesky, A., Fornito, A., Bullmore, E.T.: Network based statistic: identifying differences in brain networks. Neuroimage **53**(4), 1197–1207 (2010)
3. Kaiser, M.: A tutorial in connectome analysis: topological and spatial features of brain networks. Neuroimage **57**, 892–907 (2011)

4. Karahan, E., Rojas-Lopez, P.A., Bringas-Vega, M.L., Valdes-Hernandez, P.A., Valdes-Sosa, P.A.: Tensor analysis and fusion of multimodal brain images. Proc. IEEE **103**, 1531–1559 (2015)
5. Williams, A.H., et al.: Unsupervised discovery of demixed, low-dimensional neural dynamics across multiple timescales through tensor component analysis. Neuron (2018)
6. Destrieux, C., Fischl, B., Dale, A., Halgren, E.: Automatic parcellation of human cortical gyri and sulci using standard anatomical nomenclature. Neuroimage **53**(1), 1–15 (2010)
7. Tench, C.R., Morgan, P.S., Wilson, M., Blumhardt, L.D.: White matter mapping using diffusion tensor MRI. Magn. Reson. Med. **47**(5), 967–972 (2002)
8. Moyer, D., Gutman, B.A., Faskowitz, J., Jahanshad, N., Thompson, P.M.: Continuous representations of brain connectivity using spatial point processes. Med. Image Anal. **41**, 32–39 (2017)
9. Kolda, T.G., Bader, B.W.: Tensor decompositions and applications. SIAM Rev. **51**(3), 455–500 (2009)
10. Kiers, H.A.L.: Towards a standardized notation and terminology in multiway analysis. J. Chemometrics **14**, 105–122 (2000)
11. Yeo, B.T., et al.: The organization of the human cerebral cortex estimated by intrinsic functional connectivity. J. Neurophysiol. **106**(3), 1125–65 (2011)
12. Kolda, Tamara G.: Multilinear operators for higher-order decompositions, Technical report 2081. SANDIA, Albuquerque, NM (2006)
13. Fisher, R.A.: The use of multiple measurements in taxonomic problems. Ann. Eugenics **7**, 179–188 (1936)
14. Onnela, J.P., Saramäki, J., Kertész, J., Kaski, K.: Intensity and Coherence of motifs weighted complex networks. Phys. Rev. E. **71**(6), 065103 (2005)
15. Boccaletti, S., Latora, V., Moreno, Y., Chavez, M., Hwang, D.-U.: Complex networks: structure and dynamics. Phys. Rep. **424**(4–5), 175–308 (2006)
16. Humphries, M.D., Gurney, K.: Network small-world-ness: a quantitative method for determining canonical network equivalence. PLOS ONE **3**(4), 110,04 (2008)
17. Seeley, W.W., Crawford, R.K., Zhou, J., Miller, B.L., Greicius, M.D.: Neurodegenerative diseases target large-scale human brain networks. Neuron **62**, 42–52 (2009)
18. Zhang, H., Schneider, T., Wheeler-Kingshott, C.A., Alexander, D.C.: NODDI: practical in vivo neurite orientation dispersion and density imaging of the human brain. Neuroimage **61**, 1000–1016 (2012)